JOURNAL OF MATERIALS SCIENCE **38** (2003) 437–444

Investigation of Zr-incorporated mesoporous titania materials via nonsurfactant templated sol-gel route: Synthesis, characterization and stability

JIN-YU ZHENG, KUN-YUAN QIU*
Department of Polymer Science & Engineering, College of Chemistry & Molecular Engineering, Peking University, Beijing 100871, People's Republic of China
E-mail: kyqiu@chem.pku.edu.cn

YEN WEI*
Department of Chemistry, Drexel University, Philadelphia, PA 19104, USA
E-mail: weiyen@drexel.edu

The synthesis of Zr-incorporated mesoporous titania materials was achieved by a HCl-catalyzed nonsurfactant templated sol-gel process, followed by solvent extraction to remove the urea template. The materials were characterized by FT-IR, X-ray energy dispersive spectroscopy (XEDS), nitrogen adsorption-desorption measurement (BET), powder X-ray diffraction (XRD) and transmission electron microscopy (TEM). Zirconia has been successfully incorporated into the skeleton of titania and the observed Zr/Ti compositions are close to the designed Zr/Ti molar ratios in the feeds. The content of zirconia has significant effects on the mesoporosity and the pore parameters as well as the thermal and hydrothermal stabilities of the materials. Anatase crystal structures were formed in the materials with low Zr/Ti molar ratios. As the Zr/Ti ratio is increased, the content of anatase structures decreases and the material becomes essentially amorphous at the Zr/Ti ratio of 1/1. The materials have narrowly distributed average pore diameters in the range of 2.5–5.1 nm and disordered pore or channel structures. The incorporation of Zr increases the thermal stability but decreases the hydrothermal stability of the materials.

1. Introduction

Mesoporous materials have attracted much attention in the last decade since the discovery of the M41S family of mesoporous materials [1, 2], in which quaternary ammonium surfactants were used as templates to direct the formation of mesophase in hydrothermal synthesis. Most of the research groups focus their work on the selections of template molecules, synthetic methods, syntheses of new materials as well as the practical applications in separation, catalysts and catalyst supports [3–24]. A large amount of published research work dealt with mesoporous silica materials. However, as important materials in solid-state chemistry, transition metal oxides are drawing more and more interests due to their catalytic properties. Pure mesoporous transition metal oxides, such as zirconia, titania and niobia, as well as transition metal incorporated mesoporous silica materials (e.g., Ti-Si, Cr-Si, Mn-Si), have been prepared through various surfactant-templated hydrothermal method or modified sol-gel process [15–24]. Titania is a valuable catalyst widely used in photocatalytic reactions [25–28]. Antonelli and Ying firstly reported the preparation of mesoporous titania materials Ti-HMS1 [17]. Many groups have described the synthesis of mesoporous zirconia materials [5–8] because of their special acid catalytic character [29].

Different synthesis methods may result in different structures and thermal and hydrothermal stabilities of the resultant materials. Many works were proceeded in how to increase the thermal and hydrothermal stabilities from the view of the structures and the synthesis methods [30–36]. Incorporation of metal oxides into the skeleton of silica, such as Al, was always used to increase thermal stabilities. There have been many metal oxides doped into the silica skeleton. Others exploit organic reactions to introduce some special functional groups or hydrophobic groups to increase their hydrothermal stabilities. To our knowledge, the stabilities of some metal oxides themselves are not very

*Authors to whom correspondence should be addressed.

good. Most of the mesoporous metal oxides prepared by surfactant templated route have to be calcined at high temperature to eliminate the template molecules. As a result, the resultant porous materials always collapse during the calcination process, especially for transition metal oxides. So to some extent, the instability of pure mesoporous metal oxides limits their practical usage and finding more effective synthesis methods is necessary. Neutral surfactants or block copolymers are becoming more and more attractive in the synthesis of mesoporous metal oxides because they can be easily removed by solvent extraction, in which the collapse of the pores induced by high temperature can be avoided effectively. The synthesis of binary metal oxides is another useful way to improve the stabilities of pure metal oxides. In 1998, Elder *et al*. reported the synthesis of zirconia-stabilized mesoporous titania materials using surfactant as template and hydrothermal synthesis method [37].

Recently, Wei *et al*. reported a facile, low-cost, environmental friendly, nonsurfactant templated approach to synthesize mesoporous materials [38]. Mesoporous silica materials have been obtained by HCl-catalyzed sol-gel reactions in the presence of nonsurfactant compounds, such as D-glucose [38–41]. Mesoporous silica and titania materials were also prepared through the same approach by using urea as templates [41, 42]. Ti-incorporated mesoporous silica and Si-incorporated mesoporous titania have also been achieved via the nonsurfactant templated route. Because of some special properties of both titania and zirconia, in this article, the synthesis of Zr-incorporated mesoporous titania materials was achieved via the co-hydrolysis and co-condensation reactions of titanium (IV) *n*-butoxide (TBT) and zirconium (IV) *n*-butoxide (ZBT) in the presence of urea, which functions as a nonsurfactant template in the sol-gel reactions and is subsequently removed by solvent extraction. The mesoporosity and the pore parameters of the materials were dependent on the Zr/Ti molar ratios. The materials prepared with low Zr/Ti ratios have anatase crystal structures and amorphous natures can be formed at high Zr/Ti ratios. The incorporated titania materials exhibit disordered pore or channel structures and some accumulated interparticulate pores can also be discovered in the obtained materials. The incorporation of Zr increases the thermal stability of the materials, but decreases their hydrothermal stability.

2. Experimental section

2.1. Chemicals

Titanium (IV) *n*-butoxide (97%) and zirconium (IV) *n*-butoxide (80 wt% solution in 1-butanol) were purchased from Aldrich Chemical Company. Urea was the product of Fisher Scientific Company. All the chemicals were used without further purification.

2.2. Preparation of Zr-incorporated mesoporous titania materials

Titanium (IV) *n*-butoxide (TBT) was dissolved in ethanol at a weight ratio of 1/7. Then appropriate amount of zirconium (IV) *n*-butoxide (ZBT) was added dropwise into the TBT ethanol solution according to the designed molar ratio of Zr/Ti (i.e., 1/100 to 1/1) and stirred for 10 min. Different from the preparation of pure mesoporous titania materials [42], 12 $molL^{-1}$ and 0.28 $molL^{-1}$ HCl aqueous solutions ([TBT + ZBT]: [HCl] = 100: 1 molar ratio) were added step-by-step to hydrolyze the mixed solution of TBT and ZBT for 5 h at ambient temperature to obtain a transparent solution (sol). Then, amount of urea-ethanol-H_2O (1/5/1 weight ratio) mixed solution, with 10 wt% template content with the assumption of the complete conversion of TBT and ZBT to TiO_2 and ZrO_2, was introduced into the hydrolyzed sol under vigorous stirring and was kept stirring for another 2 h. The template-containing solution was left to stand at ambient temperature to gel and age. For sample ZT-3 (Zr/Ti = 1/20 molar ratio), 0.21 g ZBT 1-butanol solution was added to 24.1 g TBT ethanol solution and stirred for 10 min. The mixed solution was hydrolyzed by both 0.008 mL 12 $molL^{-1}$ HCl and 0.33 mL 0.28 $molL^{-1}$ HCl solution for 5 h. A urea-ethanol-H_2O solution (0.591 g) was added to serve as template or pore-forming agent. The transparent urea-containing zirconia-titania materials obtained after gelling and aging for 20–30 days were grounded into fine powder and extracted with water for 3 days to remove urea molecules. The porous Zr-incorporated titania materials were afforded after drying at 100°C for one day. As a comparison, a controlled pure TiO_2 sample with 10 wt% urea content (TBT-10) was prepared under the same conditions.

2.3. Treatment procedures of Zr-incorporated mesoporous titania materials

The extracted samples used to characterize the thermal stability were heated in oven at 350°C for 6 h with increasing rate of 1°/min and kept in oven at 100°C for 24 h with decreasing rate of 5°/min, finally cooled to room temperature. For hydrothermal treatment, the dried powder samples after solvent extraction were boiled in water for 6 h and separated, then dried at 100°C for one day.

2.4. Characterization methods

FT-IR was performed on a Bruker Vector22 FT-IR spectrometer to examine the complete removal of template molecules. The final composition of the Zr-incorporated porous titania materials with different Zr/Ti molar ratio was confirmed by X-ray energy dispersive spectroscopy (XEDS) recorded on an upgraded EDAX 9100-60 instrument, which is attached on a JEOL JEM-200CX transmission electron microscopy. The used beam spot size was 0.1 μm and the analysis was taken in the areas about 1.0 μm on the samples. The measurements were proceeded on different areas of the samples and the final composition was the average of all the measured values. The finely grounded sample powders were dissolved in ethanol solution, then one drop of the suspension was put onto a copper grid coated with a holey carbon film and dried at ambient temperature. Nitrogen adsorption-desorption isotherms were measured on a Micromeritics ASAP2010 analyzer at

−196°C via 69 points full analysis. The samples were degassed at 110°C under 1 Pa for 4 h before isotherm measurements. The pore size distributions were calculated from the desorption branches of the isotherms using Barrett-Joyner-Halenda (BJH) method. The crystal phases of the obtained materials were determined by small-angle and wide-angle powder X-ray diffraction patterns on a Rigaku DMAX2400 X-Ray Diffractometer at 40 kV and 100 mA using Cu K_α radiation ($\lambda = 0.15418$ nm). The sample scans were collected in the ranges of 2θ value of 0.6–8° and 8–60° at scan rates of 1°/min and 8°/min, respectively. The morphologies of the Zr-incorporated porous titania materials were characterized by a JEOL JEM-200CX transmission electron microscopy with an accelerate voltage of 200 kV. The preparation of the samples was same to that of X-ray energy dispersive spectroscopy.

3. Results and discussion

The synthesis of Zr-incorporated porous titania materials with various Zr/Ti molar ratios was achieved at ambient temperature in the presence of urea molecules, followed by the extraction with distilled water. The FT-IR results examined before and after water extraction confirm the complete removal of urea molecules. The absence of the bands in the range of 3300–3450 cm^{-1} and 1644 cm^{-1} ascribed to NH_2 and C═O groups in the extracted sample indicates the complete removal of urea molecules after extraction. The band at 1636 cm^{-1} in the extracted sample is attributed to the O─H bonds of H─O─H molecules in the obtained materials or KBr pallet.

The XEDS analysis results of the Zr-incorporated porous titania materials are summarized in Table I. As seen from Table I, the observed Zr/Ti molar ratios are close to the designed compositions in the feeds. This result obtained from the average method confirms the successful incorporation of zirconia into the skeleton of titania. At high Zr/Ti ratios the observed value is somewhat larger than the designed feed. It might be attributed to the higher hydrolysis and condensation rates of ZBT [43]. The XEDS pattern for sample ZT-6 is shown in Fig. 1. The peaks appeared at 4.54 keV and 15.77 keV are the typical Kα patterns of Ti and Zr. The observed Zr/Ti ratio was calculated from the ratio of the peak areas of Zr(Kα) and Ti(Kα) after the deduction of backgrounds. The 8.0 keV peak is the pattern of Cu(Kα) that is the copper grid used for supporting the samples for XEDS analysis.

The nitrogen adsorption-desorption isotherms and BJH pore size distribution plots of the samples after extraction are shown in Fig. 2. All the samples except ZT-6 have type IV isotherms with H2 hysteresis loops specific isotherm plots for mesoporous materials (Fig. 2a).

TABLE I Composition of the Zr-incorporated mesoporous titania materials with various Zr/Ti molar ratios based on XEDS analysis

Sample code		ZT-1	ZT-3	ZT-6
Zr/(Zr + Ti) (mol%)	Calculated[a]	0.99	4.76	50.0
	Observed	0.98	6.2	52.8

[a]The designed Zr content is calculated from the feed composition.

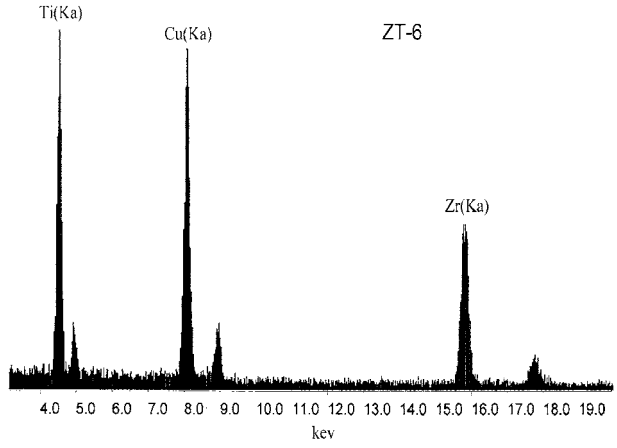

Figure 1 XEDS pattern for sample ZT-6 after the removal of urea molecules.

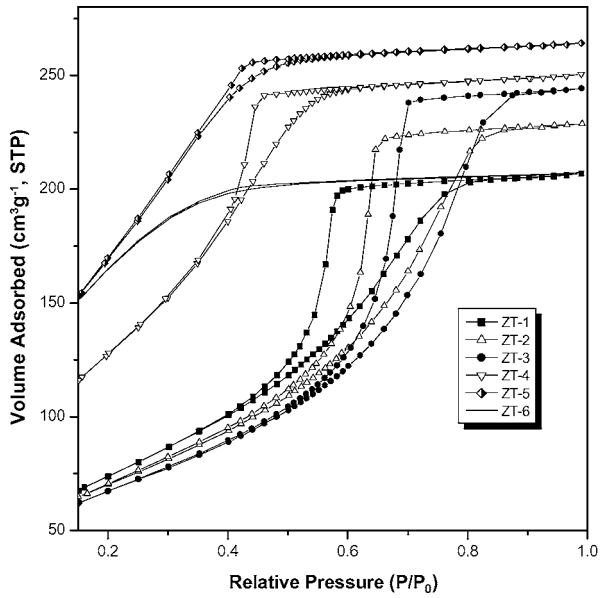

(a)

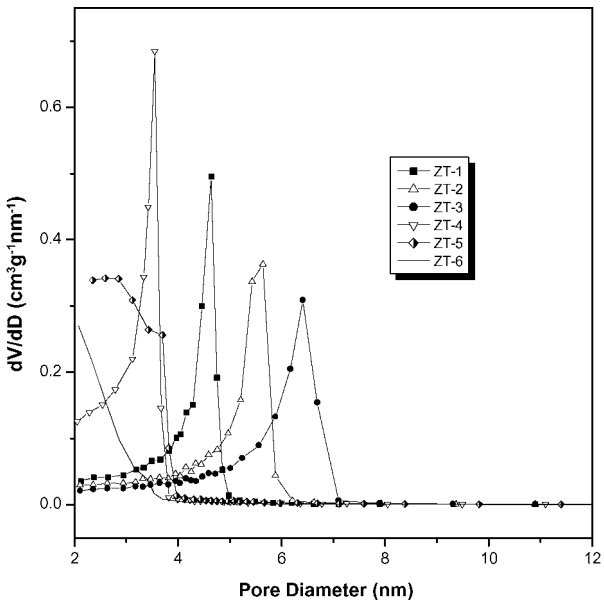

(b)

Figure 2 Nitrogen adsorption-desorption isotherms (a) and BJH pore size distribution plots calculated from desorption branches of the isotherms (b) for the Zr-incorporated mesoporous titania materials after water extraction.

TABLE II Physicochemical sorption properties and pore parameters of the samples prepared with 10 wt% template content and different Zr/Ti molar ratios

Sample code[a]	Zr/Ti molar ratio	BET surface area (m^2g^{-1})	BJH surface area (m^2g^{-1})	SP pore volume[b] (cm^3g^{-1})	Total pore volume[c] (cm^3g^{-1})	Average pore diameter[d] (nm)	Peak pore diameter[e] (nm)
TBT-10	0	223.7	294.7	0.306	0.303	4.1	4.8
ZT-1	1/100	264.6	347.1	0.320	0.333	3.8	4.6
ZT-2	1/50	243.9	325.7	0.354	0.365	4.5	5.6
ZT-3	1/20	229.9	304.8	0.378	0.386	5.1	6.4
ZT-4	1/10	516.7	567.6	0.388	0.429	3.0	3.6
ZT-5	1/4	633.4	672.2	0.409	0.499	2.9	–
ZT-6	1/1	466.6	361.9	0.321	0.227	2.5	–

[a]All the samples were synthesized at 10 wt% template content with the assumption of the complete conversion of TBT and ZBT to TiO_2 and ZrO_2.
[b]Single point (SP) pore volume was measured at $P/P_0 \approx 1$.
[c]Total pore volume of pores with 1.7–300 nm diameters was calculated from Barrett-Joyner-Halenda (BJH) method.
[d]Average pore diameter was obtained from the BJH method based on desorption branches of the isotherms.
[e]The peak pore diameter was the peak value of the BJH pore size distribution plot.

The mesoporosity of the samples is very significant at low Zr/Ti molar ratios (i.e., ZT-1–3). When the Zr/Ti molar ratio is increased to such as 1/10–1/4, the H2 hysteresis loops become smaller. Type I reversible isotherm typical for a microporous material was observed in sample ZT-6 with 1/1 Zr/Ti ratio. The adsorbed volumes at $P/P_0 \approx 1$ have an increase tendency with increased Zr/Ti ratios. This tendency is in agreement with the data listed in Table II. The relative pressures corresponding to the hysteresis loops in the desorption-isotherms increase first and then shift to lower values, which identify the changes of the average pore diameters. From Fig. 2b we can see, the widths at the half peak heights, identifying the distributions of average pore diameters, are relatively narrow; moreover, the peak pore diameters can increase to about 6.5 nm. But at Zr/Ti ratios of 1/4 and 1/1, there is no identifiable distribution peak.

Table II presents the physicochemical sorption properties and pore parameters of the samples prepared with 10 wt% template content and different Zr/Ti molar ratios. The surface areas calculated either by Brunauer-Emmett-Teller (BET) method or by Barrett-Joyner-Halenda (BJH) method decrease first with the increase of Zr/Ti molar ratio from 1/100 to 1/20 and then go up from 1/20 to 1/4. The average pore diameter obtained from BJH method based on desorption branches of the isotherms increases from 3.8 nm to 5.1 nm as the Zr/Ti ratio is increased from 1/100 to 1/20 and then decreases to 2.5 nm with the molar ratio increasing to 1/1. The pore volumes keep increasing when the molar ratio is increased from 1/100 to 1/4. However, both surface area and pore volume decrease significantly at the Zr/Ti ratio of 1/1, which might be induced either by the phase separation during aging process or by higher hydrolysis and condensation rates of ZBT. The powder XRD patterns measured on the samples before water extraction, reveal that no phase separation happened in aging process even with high Zr incorporation content. There is no any diffraction peak corresponding to urea crystals, which has a sharp diffraction peak at 22.2° and some peaks at 24.5°, 29.2° and 35.5° etc., can be examined. The higher hydrolysis and condensation rates of ZBT are perhaps the main factor leading to the decrease of surface area and pore volume. Comparing to the control sample TBT-10, the incorporation of Zr results in the increase of pore volumes and the adjusting of pore diameters.

The incorporation of Zr into titania skeleton leads to significant changes of the thermal and hydrothermal stabilities. Table III presents the sorption properties and pore parameters of pure titania sample and Zr-incorporated titania samples after thermal and hydrothermal treatments. Pure titania sample (TBT-10) has good hydrothermal stability. The changes of pore

TABLE III Physicochemical sorption properties and pore parameters of the samples before and after thermal and hydrothermal treatments

Sample code[a]	Zr/Ti molar ratio	BET surface area (m^2g^{-1})	BJH surface area (m^2g^{-1})	SP pore volume (cm^3g^{-1})	BJH pore volume (cm^3g^{-1})	Peak pore diameter[b] (nm)
TBT-10	0	223.7	294.7	0.306	0.303	4.8
TBT-10-O	0	159.1	226.9	0.271	0.265	5.5
TBT-10-B	0	193.1	262.7	0.266	0.275	4.9
ZT-1	1/100	264.6	347.1	0.320	0.333	4.6
ZT-1-O	1/100	195.1	276.9	0.298	0.304	4.9
ZT-1-B	1/100	239.0	321.7	0.313	0.323	4.9
ZT-3	1/20	229.9	304.8	0.378	0.386	6.4
ZT-3-O	1/20	169.3	243.0	0.359	0.362	7.2
ZT-3-B	1/20	171.7	236.5	0.349	0.353	7.4
ZT-4	1/10	516.7	567.6	0.388	0.429	3.6
ZT-4-O	1/10	372.7	426.1	0.296	0.318	3.4
ZT-4-B	1/10	168.5	233.3	0.339	0.343	7.4

[a]In the sample's code, the "O" means thermal treatment with oven at 350°C, and the "B" indicates hydrothermal treatment in boiling water.
[b]The peak pore diameter was the peak value of the BJH pore size distribution plot.

diameter and surface area after hydrothermal treatment are slight. But the pore diameters of Zr-incorporated samples after hydrothermal treatment increase significantly with the increased incorporation content of Zr. This is proposed that the increase of the hydrophilic properties after the introduction of Zr into titania skeleton makes the skeleton become more instable in the presence of hot water. After thermal treatments, the changes of pore parameters for Zr-incorporated samples are relatively smaller than those of pure titania sample, indicating the increase of thermal stability with the incorporation of Zr. However, the increase of thermal stability is not linearly dependent on the incorporation content of Zr. Comparing all the parameters, low incorporation content of Zr is relatively effective for the increase of thermal stability. From the view of pore diameter, the increase of thermal stability is more pronounced at high incorporation content of Zr, in which the pore diameter almost unchanges after treatments. The dispersion of Zr in the skeleton of titania and the formation of Zr—O—Ti networks strengthen the skeleton and lead to the increase of thermal stability.

The N_2 adsorption-desorption isotherms for samples ZT-1 and ZT-4 after thermal and hydrothermal treatments are shown in Fig. 3. The samples after thermal and hydrothermal treatments are still mesoporous materials. However, the relative pressures corresponding to the hysteresis loops shift to high values after treatments suggesting the increase of pore diameters. As for the effect of thermal treatment, the shifted values become smaller as the incorporation content of Zr is increased, which identify that the thermal stabilities of the materials increase with the increased incorporation content of Zr. For hydrothermal treatment, the values of hysteresis loops go up to higher values too; however, the changes become more obvious, indicating the increase of pore diameters and the decrease of hydrothermal stability. These are mainly because of the increase of

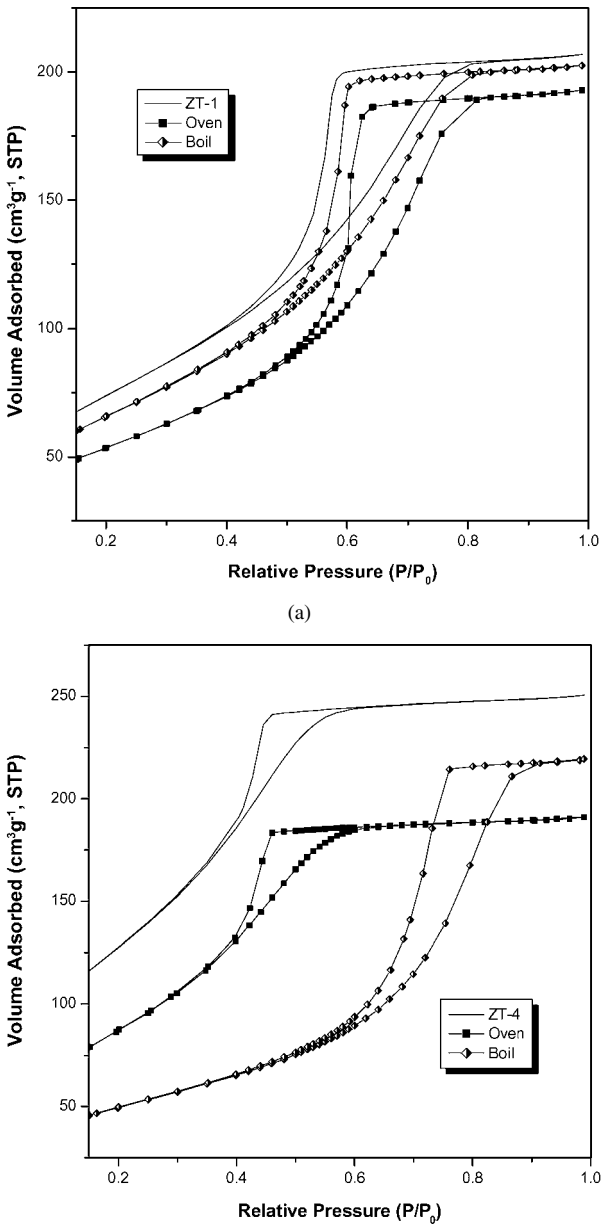

Figure 3 Nitrogen adsorption-desorption isotherms for samples ZT-1 (a) and ZT-4 (b) before and after treatments.

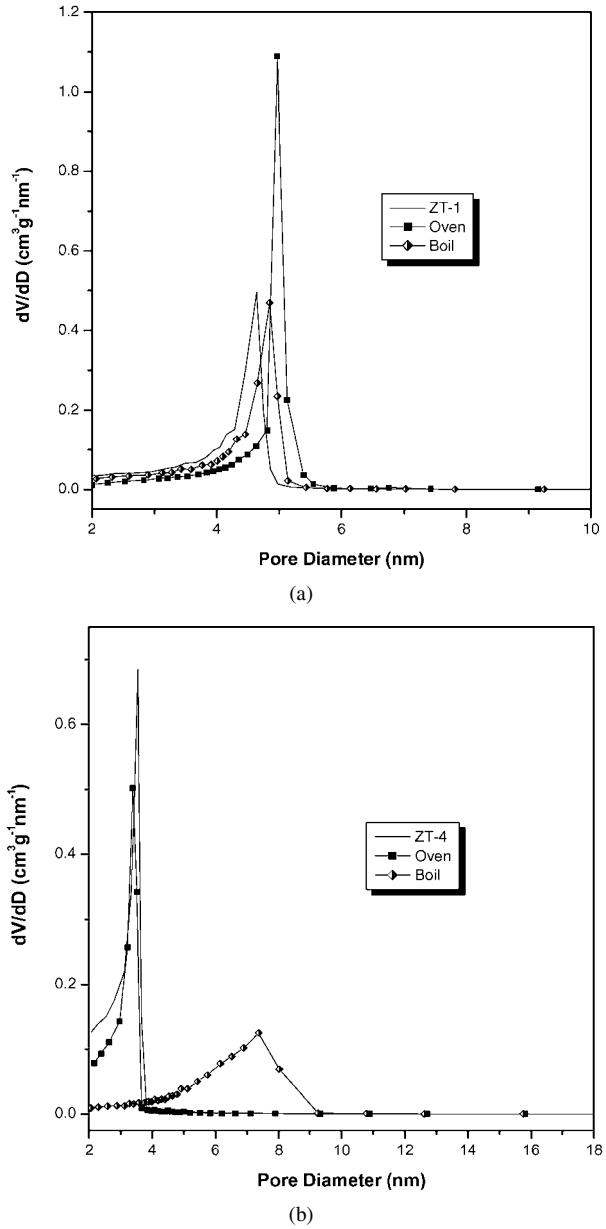

Figure 4 BJH pore size distribution plots calculated from desorption branches of the isotherms for samples ZT-1 (a) and ZT-4 (b) before and after treatments.

hydrophilic properties of Zr-incorporated samples and the collapse of pore walls.

Fig. 4 shows the corresponding BJH distribution plots of the samples after thermal and hydrothermal treatments, obtained from the desorption branches of the isotherms. The peaks of pore diameters shift to high values after treatments, which indicates the increase of thermal stabilities and the decrease of hydrothermal stabilities of the samples. The half widths of the distribution peaks for thermal treated samples are very narrow and almost do not change after treatment; however, the widths after hydrothermal treatments become broader, indicating the decrease of hydrothermal stabilities and the uneven distribution.

Fig. 5 shows the small-angle (2θ: 0.6–8°) and wide-angle (2θ: 8–60°) powder X-ray diffraction patterns for the extracted samples. Sample ZT-1 only has one wide diffraction peak centered at 2θ value of 0.96°. There is no other diffraction peak found in higher 2θ values, suggesting the lack of long-range ordered arrangements. For sample ZT-3, there is a weak, broad peak at 2θ value around 1.7°. At higher Zr/Ti ratios, no any diffraction peak appears, which indicate the disordered arrangements. In the wide-angle XRD patterns, Zr-incorporated mesoporous titania materials with anatase structures are obtained at low Zr/Ti ratios (e.g., ZT-1, ZT-3 and ZT-4). However, the intensities of the

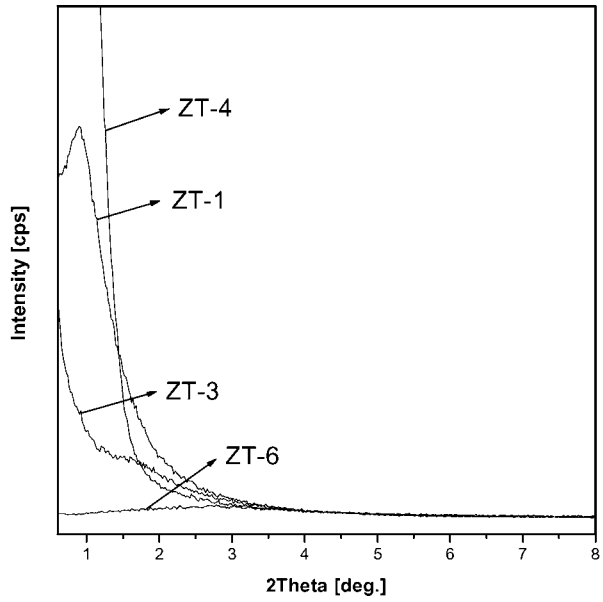

(a)

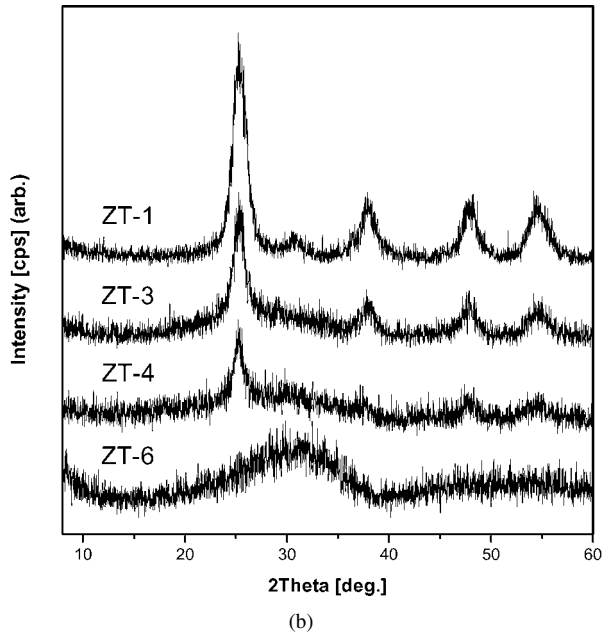

(b)

Figure 5 Small-angle (a) and wide-angle (b) powder X-ray diffraction patterns for samples ZT-1, ZT-3, ZT-4 and ZT-6.

(a)

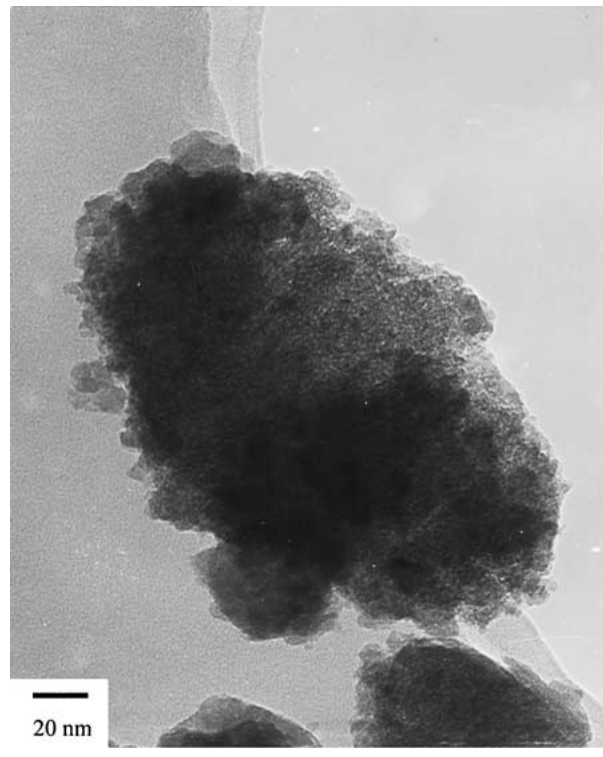

(b)

Figure 6 TEM images for samples ZT-1 (a) and ZT-4 (b) after removal of urea molecules and sample ZT-1-H (c) after thermal treatment. (*Continued.*)

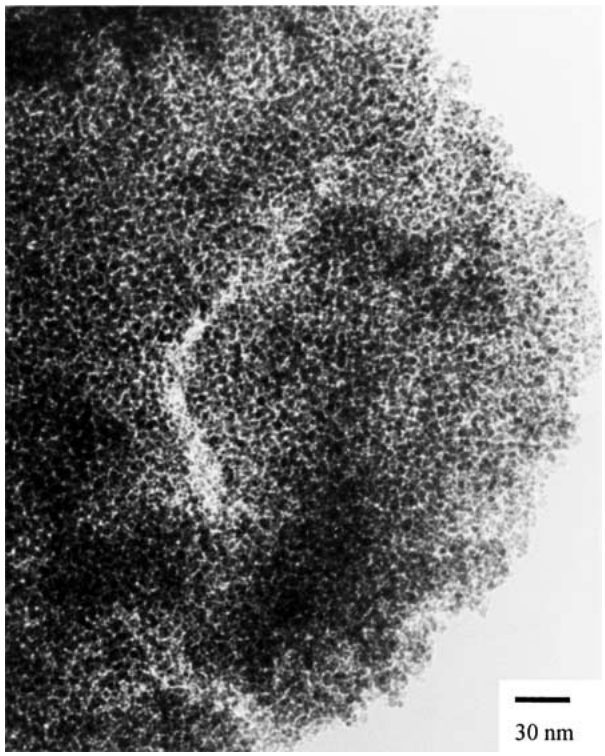

(c)

Figure 6 (*Continued*).

crystal peaks identifying the anatase structures, with 2θ values of 25°, 38°, 48° and 54.5°, become weaker with the increase of Zr/Ti ratio. In sample ZT-6, no crystal peaks of anatase structure was found and there was only one broad peak appeared at 2θ value of about 32°, indicating the amorphous natures of the sample with 1/1 Zr/Ti ratio. This is probably ascribed that the uniform dispersion of Zr in the titania skeleton disrupts the anatase structures of titania. However, after thermal treatment, the anatase structure of sample ZT-4 becomes clear that perhaps because the thermal treatment induces the deep crystallization of titania skeleton.

The TEM images for samples ZT-1 (a), ZT-4 (b) and thermal treated sample ZT-1-H (c) are shown in Fig. 6. The materials possess numerous interconnected wormhole-like channels. However, there is no long-range ordered pore and channel structures. Moreover, it is much easier to find porous structures for the samples prepared with high Zr/Ti ratios, e.g. ZT-4. In ZT-1, some particles appear to accumulate tightly together to form interparticulate pores, which maybe another reason leading to the absence of diffraction peaks in small-angle scales of XRD patterns. After thermal treatment, the accumulation of the particles is more apparent. The pores or channels connected together.

4. Conclusions

In this article, we have presented the synthesis of Zr-incorporated mesoporous titania materials via HCl-catalyzed sol-gel reactions by using urea as nonsurfactant template (or pore-forming agent) followed by solvent extraction. The XEDS results identify that zirconia has been incorporated into the skeleton of titania with close compositions to the designed feeds. The mesoporosity of the materials is pronounced related to the incorporation content of zirconia. The average pore diameter increases from 3.8 nm to 5.1 nm and then decreases to 2.5 nm, when the Zr/Ti ratio is increased from 1/100 to 1/20 and from 1/20 to 1/1. XRD results reveal that the materials possess anatase crystal structures at 1/100–1/10 Zr/Ti ratios. The materials lack long-range ordered pore and channel structures based on the XRD patterns and TEM images. The even dispersion of Zr in titania skeleton and high hydrolysis and condensation rates of ZBT as well as the hydrogen bonding interactions between the hydrolyzed Ti─OH or Zr─OH and the aggregates of urea molecules are supposed to play significant roles in the preparation of Zr-incorporated mesoporous titania materials. The measurement results also indicate that the incorporation of Zr into titania skeleton increases thermal stability but decreases hydrothermal stability of these binary mesoporous materials.

Acknowledgements

This work is supported by the National Nature Science Foundation of China through a grant to K. Y. Qiu (No. 29874002) and an Outstanding Young Scientist Award to Y. Wei (No. 29825504). Y. Wei is also grateful to US Army Research Office (ARO-STIR No. 41495-II) for partial support of this project. We thank Prof. X. H. Chen (Institute of Materials Science, Tsinghua University) for her kind assistance in the TEM measurements.

References

1. C. T. KRESGE, M. E. LEONOWICZ, W. J. ROTH, J. C. VARTULI and J. S. BECK, *Nature* **359** (1992) 710.
2. J. S. BECK, J. C. VARTULI, W. J. ROTH, M. E. LEONOWICZ, C. T. KRESGE, K. D. SCHMITT, C. T.-W. CHU, D. H. OLSON, E. W. SHEPPARD, S. B. MCCULLEN, J. B. HIGGINS and J. L. SCHLENKER, *J. Am. Chem. Soc.* **114** (1992) 10834.
3. Q. HUO, D. I. MARGOLESE, U. CIESLA, P. FENG, T. E. GIER, P. SIEGER, R. LEON, P. M. PETROFF, F. SCHUTH and G. D. STUCKY, *Nature* **368** (1994) 317.
4. U. CIESLA, D. DEMUTH, R. LEON, P. M. PETROFF, G. STUCKY, K. UNGER and F. SCHUTH, *J. Chem. Soc. Chem. Commun.* (1994) 1387.
5. U. CIESLA, S. SCHACHT, G. D. STUCKY, K. K. UNGER and F. SCHUTH, *Angew. Chem. Int. Ed. Engl.* **35** (1996) 541.
6. P. LIU, J. S. REDDY, A. ADNOT and A. SAYARI, *Mater. Res. Soc. Symp. Proc.* **431** (1996) 101.
7. M. S. WONG, D. M. ANTONELLI and J. Y. YING, *Nanostr. Mater.* **9** (1997) 165.
8. M. S. WONG and J. Y. YING, *Chem. Mater.* **10** (1998) 2067.
9. A. FIROUZI, F. ATEF, A. G. OERTLI, G. D. STUCKY and B. CHMELKA, *J. Am. Chem. Soc.* **119** (1997) 3596.
10. D. ZHAO, Q. HUO, J. FENG, B. F. CHMELKA and G. D. STUCKY, *ibid.* **120** (1998) 6024.
11. D. ZHAO, J. FENG, Q. HUO, N. MELOSH, G. H. FREDRICKSON, B. F. CHMELKA, and G. D. STUCKY, *Science* **279** (1998) 548.
12. D. ZHAO, P. YANG, D. I. MARGOLESE, B. F. CHMELKA and G. D. STUCKY, *Chem. Commun.* (1998) 2499.
13. P. T. TANEV and T. J. PINNAVAIA, *Science* **267** (1995) 865.
14. S. A. BAGSHAW, E. PROUZET and T. J. PINNAVAIA, *ibid.* **269** (1995) 1242.
15. W. ZHANG, B. GLOMSKI, T. R. PAULY and T. J. PINNAVAIA, *Chem. Commun.* (1999) 1803.
16. Y. H. YUE, Z. MA, W. M. HUA and Z. GAO, *Huaxue Xuebao* **58** (2000) 777.
17. D. M. ANTONELLI and J. Y. YING, *Angew. Chem. Int. Ed. Engl.* **34** (1995) 2014.

18. *Idem*., *ibid*. **35** (1996) 426.
19. *Idem*., *Curr. Opin. Colloid Interface Sci*. **1** (1996) 523.
20. D. M. ANTONELLI, *Micro. Meso. Mater*. **30** (1999) 315.
21. R. L. PUTNAM, N. NAKAGAWA, K. M. MCGRATH, N. YAO, I. A. AKSAY, S. M. GRUNER and A. NAVROTSKY, *Chem. Mater*. **9** (1997) 2690.
22. V. F. STONE JR. and R. J. DAVIS, *ibid*. **10** (1998) 1468.
23. M. THIEME and F. SCHUTH, *Micro. Meso. Mater*. **27** (1999) 193.
24. P. D. YANG, D. Y. ZHAO, D. I. MARGOLESE, B. F. CHMELKA and G. D. STUCKY, *Nature* **396** (1998) 152.
25. Y. LUO and D. F. OLLIS, *J. Catal*. **163** (1996) 1.
26. S. C. LUO and J. L. FALCONER, *ibid*. **185** (1999) 393.
27. L. X. CAO, A. M. HUANG, F.-J. SPIESS and S. L. SUIB, *ibid*. **188** (1999) 48.
28. L. X. CAO, Z. GAO, S. L. SUIB, T. N. OBEE, S. O. HAY and J. D. FREIHAUT, *ibid*. **196** (2000) 253.
29. T. YAMAGUCHI, *Catal. Today* **20** (1994) 199.
30. M. CHATTERJEE, T. IWASAKI, H. HAYASHI, Y. ONODERA, T. EBINA and T. NAGASE, *Catal. Lett*. **52** (1998) 21.
31. K. A. KOYANO, T. TATSUMI, Y. TANAKA and S. NAKATA, *J. Phys. Chem. B* **101** (1997) 9436.
32. T. TATSUMI, K. A. KOYANO, Y. TANAKA and S. NAKATA, *Meso. Mol. Sieves 1998 Studies in Surface Science and Catalysis* **117** (1998) 143.
33. M. M. L. R. CARROTT, A. J. E. CANDEIAS, P. J. M. CARROTT and K. K. UNGER, *Langmuir* **15** (1999) 8895.
34. N. IGARASHI, Y. TANAKA, S. NAKATA and T. TATSUMI, *Chem. Lett*. **1** (1999) 1.
35. K. YAMAMOTO and T. TATSUMI, *ibid*. **6** (2000) 624.
36. W. J. LI, Y. W. YAO, Z. C. WANG, J. Z. ZHAO, M. Y. ZHAO and C. Q. SUN, *Mater. Chem. Phys*. **70** (2001) 144.
37. S. H. ELDER, Y. GAO, X. LI, J. LIU, D. E. MCCREADY and C. F. WINDISCH JR., *Chem. Mater*. **10** (1998) 3140.
38. Y. WEI, D. JIN, T. DING, W. H. SHIH, X. H. LIU, S. Z. D. CHENG and Q. FU, *Adv. Mater*. **10** (1998) 313.
39. J. Y. ZHENG, J. B. PANG, K. Y. QIU and Y. WEI, *J. Inorg. Organomet. Polym*. **10** (2000) 103.
40. J. B. PANG, K. Y. QIU, Y. WEI, X. J. LEI and Z. F. LIU, *Chem. Commun*. (2000) 477.
41. J. B. PANG, K. Y. QIU, J. G. XU, Y. WEI and J. CHEN, *J. Inorg. Organomet. Polym*. **10** (2000) 39.
42. J. Y. ZHENG, J. B. PANG, K. Y. QIU and Y. WEI, *Micro. Meso. Mater*. **49** (2001) 189.
43. P. JUDEINSTEIN and C. SANCHEZ, *J. Mater. Chem*. **6** (1996) 511.

Received 5 April
and accepted 24 September 2002